THESIS FOR THE DEGREE OF DOCTOR OF PHILOSOPHY

Gear engagement control for transmissions in hybrid electric vehicles

MUDDASSAR ZAHID PIRACHA

CHALMERS

Department of Electrical Engineering
Division of Systems and Control
CHALMERS UNIVERSITY OF TECHNOLOGY

Göteborg, Sweden 2024

Gear engagement control for transmissions in hybrid electric vehicles

MUDDASSAR ZAHID PIRACHA
ISBN 978-91-7905-984-2

Doktorsavhandlingar vid Chalmers tekniska högskola
Ny serie nr 5450
ISSN 0346-718X

Department of Electrical Engineering
Division of Systems and Control
Chalmers University of Technology
SE-412 96 Gothenburg
Sweden
Telephone + 46 (0)31-772 1000

Email: piracha@chalmers.se; piracha.muddassar@gmail.com

Cover:
The figure on the front cover shows four control methods for minimization of synchronization time as well as noise/wear during a gear shift. Detailed explanation is provided on page 18.

Chalmers Reproservice
Gothenburg, Sweden 2024

To my family…

ABSTRACT

Hybrid and electric vehicles have become very important for vehicle manufacturers due to stricter legislation, government incentives and customers' growing awareness of the environmental issues. For conventional vehicles, Dual clutch transmissions (DCT) have better shift quality and efficiency than conventional automatic transmissions. The hybridization of a DCT leads to several challenges to the shift quality. The most important aspects of shift quality are smoothness, shift time as well as noise and wear during a shift.

This thesis presents control methods for improving shift quality in a hybridized DCT during torque interrupt shifts. During these gear shifts, the traction source is disconnected from the wheels, thus long shift times adversely affect drivability. Firstly, a method to minimize the shift time during a torque interrupt shift is presented. A simulation method is also presented which demonstrates the relationship between dog teeth contacts during a shift and noise and wear. To reduce noise and wear, model-based open-loop and model-based feedback control methods are designed that minimize the intensity of the dog teeth contact. A time-optimal control method, which minimizes both the shift time and the intensity of the dog teeth contact, is developed. Performance of the control methods is verified by simulations.

The second part of the thesis focus on a dedicated hybrid transmission (DHT). The DHT in this research is shifted from series mode to parallel mode, by the engagement of a dog clutch. To minimize noise during the mode switch, an LQI controller has been designed for the speed synchronization of the dog clutch. An algebraic method of determining the feedback gains of the LQI controller, based on the physical parameters and functional requirements of the system, has been developed, greatly reducing the need for manual tuning.

The control methods defined in this thesis focus on implementation in the existing control hardware and software, so the complex calculations are done offline and control algorithm that must be embedded in real-time systems has been kept simple. Using this approach, optimum performance from the mechanical synchronizer or dog clutch system can be achieved without extending vehicles' existing control systems.

Keywords: Hybrid Powertrain, Electric Powertrain, Dual Clutch Transmission, Dedicated Hybrid Transmission, Gear shifting, Drivability, Mechanical Synchronizers, Dog Clutch, Noise and wear minimization, Optimal control, Phase plane analysis, LQI control

List of Publications

This thesis is based on the work contained in the following appended papers:

Paper A

Improving gear shift quality in a PHEV DCT with integrated PMSM
Muddassar Zahid Piracha, Anders Grauers, Johan Hellsing
Conference contribution to CTI Symposium Automotive Transmissions, HEV and EV Drives
Berlin, Germany. Dec 2017
ISBN 978-3-9817822-3-3

Paper B

Model Based Control of Synchronizers for Reducing Impacts during Sleeve to Gear Engagement
Muddassar Zahid Piracha, Anders Grauers, Eva Barrientos, Henrique Budacs and Johan Hellsing
Paper in proceedings for SAE World Congress Experience
Detroit, USA. Apr 2019.
DOI:10.4271/2019-01-1303

Paper C

Time optimal control of gearbox synchronizers for minimizing noise and wear
Muddassar Zahid Piracha, Anders Grauers and Johan Hellsing
Paper in proceedings for 2020 IEEE Conference on Control Technology and Applications (CCTA)
DOI:10.1109/CCTA41146.2020.9206254

Paper D

Feedback Control of Synchronizers for Reducing Impacts during Sleeve to Gear Engagement
Muddassar Zahid Piracha, Anders Grauers and Johan Hellsing
Journal Article in SAE International Journal of Advances and Current Practices in Mobility 2(4) 2020
DOI:10.4271/2020-01-0960

Paper E

Model based algebraic weight selection for LQI control reducing dog clutch engagement noise
Muddassar Zahid Piracha, Anders Grauers and Johan Hellsing
To be published in proceedings for SAE World Congress Experience 2024

Additional Publications

The author has also drafted the following patent applications related to the research topic:

Improving gear shift quality in a PHEV DCT with Integrated PMSM
METHOD FOR SYNCHRONISATION OF A FIRST TRANSMISSION COMPONENT
Publication/Patent Number: EP3473894B1
Filing date: 20/10/2017

Control method to minimize noise and wear in synchronizers during gear shifts
METHOD AND SYSTEM FOR GEAR ENGAGEMENT
Publication/Patent Number: EP3647631B1
Filing date: 30/10/2018

Method for identification of drag torque coefficient
METHOD FOR DETERMINING A DRAG TORQUE COEFFICIENT
Publication/Patent Number: EP3816485B1
Filing date: 01/11/2019

Estimation of dog teeth positions for contact minimization during shifts using PMSM angle information
A METHOD FOR OPERATING A VEHICLE DRIVETRAIN
Publication/Patent Number: EP3936737A1
Filing date: 06/07/2023

Algebraic method for LQI controller calibrations
A METHOD FOR CALIBRATING FEEDBACK GAINS OF AN LQI CONTROLLER
Application number: EP23151473.8
Filing date: 13/01/2023

Acknowledgements

First and foremost, I would like to acknowledge the kind guidance, continuous support and encouragement of my supervisors Docent Anders Grauers and Johan Hellsing. This thesis owes a lot to their dedicated involvement.

I would also like to thank all my managers at CEVT Fredrik Niklasson, Petter Frejinger, Arvid Mörtzell, Anna-Karin Andersson, Hans Mark, Fangkun Lindström and Hui Zhong for all their support throughout the years. For providing me with a great working environment at CEVT, I would like to thank the Powertrain Concept, the Electric Drive and the ADAS teams. I am also deeply grateful for all the great friends and colleagues I have at Systems and Control department at Chalmers.

I would also like to thank Swedish Energy Agency for funding this project via the FFI program.

My colleagues Eva Barrientos, Henrique Budacs, Pär Freudenthaler, Tobias Berndtson and Dr. Martin Johansson deserve special thanks, from whom I have learned a lot during the years.

I am also thankful to all the amazing teachers at the department especially Prof. Bo Egardt, Prof. Claes Breitholtz, Prof. Torsten Wik and Prof. Nikolce Murgovski.

My sincerest thanks also go to Dr. Börje Grandin for all his efforts in getting this project started. The support I have received over the years from Albert Pettersson, Dr. Håkan Sandquist, Dr. Simon Klacar, Dr Shafiq Urréhman, Jens Larsen, Michael Palander, Dr. Lars Ivarsson, Fredrik Sjöqvist, Johan Jannesson, Henrik Dhejne, Torbjörn Kvist and Torgrim Brochmann is greatly appreciated.

The amazing support I received from Emil Jönrup at CEVT and Torbjörn Axelsson from Zacco with drafting of the patent applications is greatly appreciated.

A huge thanks to my friend and fellow Industrial PhD student Sepideh Amirpour for all the delightful conversations. I am deeply grateful to all my amazing colleagues and dear friends especially Dr Ankit Gupta, Omer Farooq, Shabbir Adil, Avnish Narula, Peyman Jafarian, Farhan Khan, Usman Afridi, Zain Zubair and Shiraj Shekh.

I am forever grateful to my parents, whose constant support, prayers, and unconditional love makes me who I am today. The love and encouragement from my siblings is a source of great inspiration and is gratefully acknowledged.

Above all I would like to thank my wife, Sidra for all her love and support.

Alhamdulillah for everything
Muddassar Zahid Piracha
Göteborg, January 2024

Table of Contents

Part 1: Control of Hybrid Dual Clutch Transmission

1. Rationale

When a conventional dual clutch transmission (DCT) is hybridized, CO_2 emissions from the vehicle are reduced but the hybridization also leads to some disadvantages compared with conventional DCT.

This thesis reports the results of the 7-speed hybrid DCT project (7DCTH), which aims to reduce and eliminate some of the drawbacks of hybridization. The results of the project are:

- A control method to reduce synchronization time during gear shifting of 7DCTH in electric vehicle mode (EV mode).
- A model-based open-loop and a feedback control method to avoid noise and wear of mechanical synchronizer systems (applicable to synchronizers in both hybrid and conventional DCTs).
- A time-optimal control method to minimize synchronization time, noise and wear during gear shifting in 7DCTH (also applicable to dog clutch systems).

The detailed analysis and results of the project are presented in Papers A to D. This part of the thesis provides a background to the topic, showing how the papers' results relate to each other and how they should be combined to improve the overall gear shifting of a hybrid DCT.

The control methods defined in this thesis focus on implementing the control methods in existing control hardware and software. Thus, all complex calculations are done offline and the control algorithm that must be embedded in real-time systems is kept simple.

2. Dual Clutch Transmissions

A conventional 7-speed dual clutch transmission is shown in Figure 1. The internal combustion engine (ICE) is connected to wheels via an odd clutch (C1) and even clutch (C2) and their respective gear pairs.

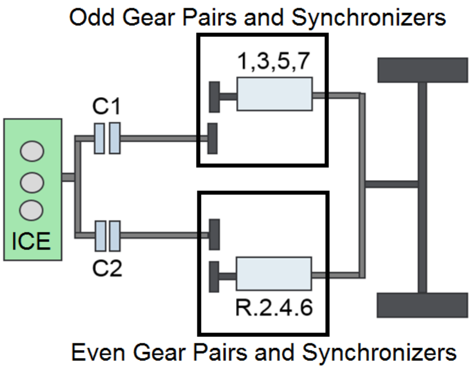

Figure 1 Conventional DCT

It can be seen in Chapter 5 of [1] that DCT has the lowest losses compared with both an automatic transmission and a continuously variable transmission. The high efficiency of DCT is owing to its mechanical similarity to a manual transmission. A manual transmission is shown in Figure 2.

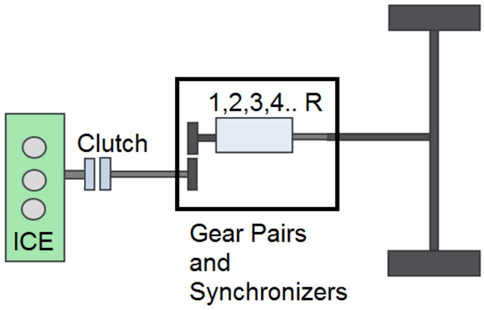

Figure 2   Manual Transmission

A conventional DCT, shown in Figure 1, can be seen as two manual transmissions connected in parallel. Thus, a DCT has almost the same efficiency as a manual transmission and offers operational convenience similar to conventional automatic transmissions [2]. Moreover, in a DCT, gear shifting is smooth and without torque interrupts, as compared with a manual transmission, as shown by Figure 3.

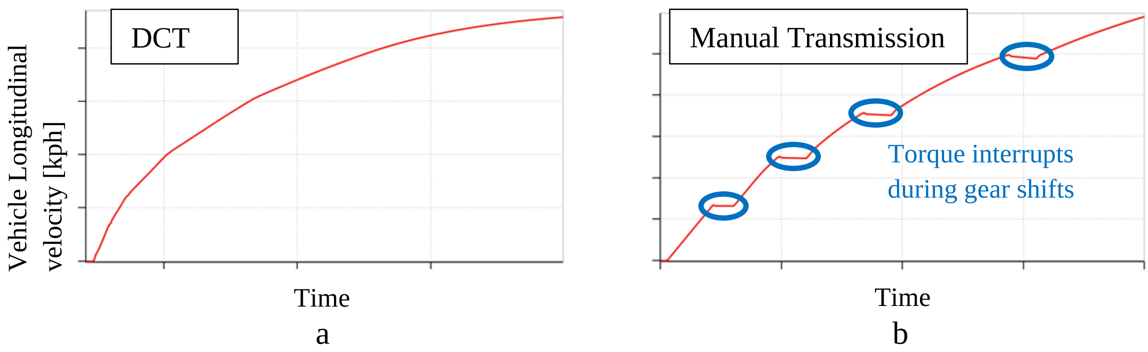

Figure 3   Vehicle speed with respect to time during an acceleration maneuver a) for a DCT b) for a manual transmission

When a gear is to be changed in a manual transmission, the driver disengages the clutch, changes gear and then engages the clutch to continue driving. So, during gear shift, the ICE is disconnected from the wheels and consequently, the vehicle does not accelerate. This is shown by blue circles in Figure 3b. This particular kind of shift is known as a “torque interrupt shift” because propulsion torque is interrupted during the gear shift.

A gear shift in a DCT, for instance a shift from an odd gear to an even gear, only requires clutch C1 to be disengaged while clutch C2 is engaged; hence ICE delivers a continuous torque to the wheels. The driver, therefore, feels a continuous acceleration during gear shifts, as shown by the smoothly increasing velocity profile in Figure 3a. A torque interrupt shift is not a part of normal driving for DCT and is only used if some part of the transmission has a failure for example one of the clutches or one of the shafts is unavailable.

3. Hybrid Dual Clutch Transmissions

Increasingly stringent requirements to reduce CO_2 emissions are making vehicle electrification a necessary measure for the future. Various hybrid concepts can be chosen based on conventional DCTs, mainly by connecting an electric motor (EM) to the transmission in different ways. Figure 4 shows the concept chosen by China Euro Vehicle Technology AB (CEVT). The traction EM is integrated into the DCT and is connected to the shaft from clutch 2 to the even gear pairs. There is no way of disconnecting the traction EM from the DCT.

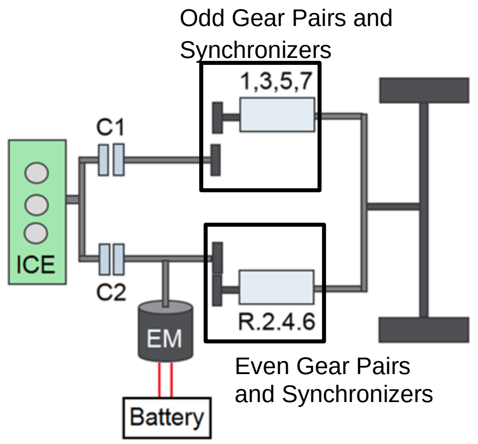

Figure 4 Hybrid DCT

The 7-speed hybrid DCT shown in Figure 4 has the following advantages over other hybrid DCT concepts:

- 7DCTH fits within conventional platform because it leads to least number of platform changes. Thus, this concept is cheaper, because a lot of components can be carried over from the conventional powertrain.
- It has only one electric motor and, hence costs less than many other PHEV transmission concepts with multiple electric motors in the powertrain. One such transmission with multiple electric motors is the dedicated hybrid transmission which is discussed in detail in the later part of this thesis.
- Compared with another hybrid DCT concept shown in Figure 5, the 7DCTH concept costs less. This is because the other concept requires another clutch to be added into the system and major platform changes to the vehicle.

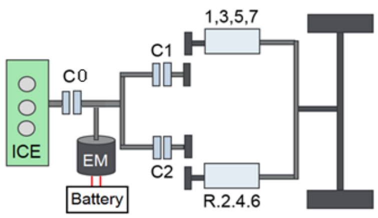

Figure 5 Hybrid DCT concept with electric motor connected between ICE and DCT

- Compared with a pure electric vehicle, it has a smaller battery and electric powertrain because ICE will also provide traction power to the wheels. Hence, the cost of powertrain electrification is low.

Since 7DCTH has two power sources, it can operate in many different modes, depending on whether the ICE or EM is delivering the traction power, or both. The EM can also be used as a generator to charge the battery, which adds even more modes.

If both the ICE and EM provide traction power simultaneously, the powertrain operates in Hybrid driving mode. The power flow in 7DCTH in hybrid driving mode is indicated by yellow lines in Figure 6.

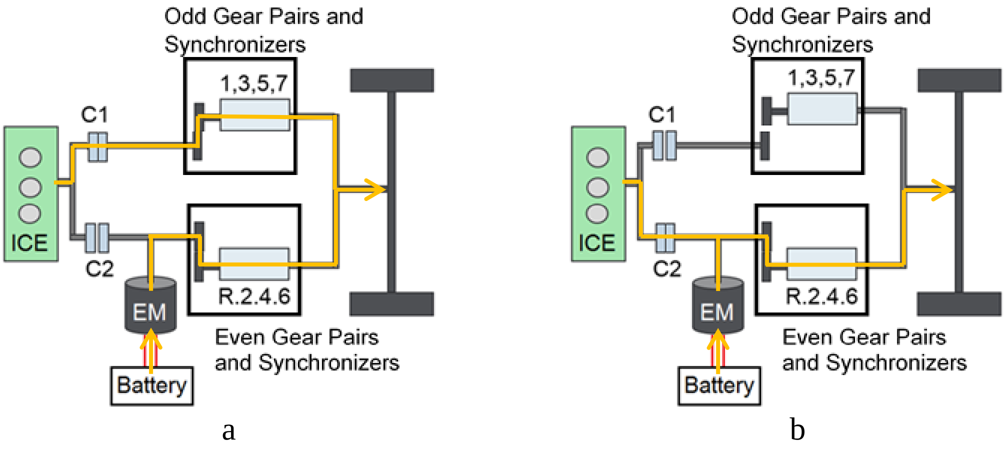

Figure 6 Hybrid Driving mode in 7DCTH when a) ICE uses odd gears and b) ICE uses even gears.

Figure 6a shows hybrid driving mode when the ICE is using odd gears. Figure 6b shows the ICE is using even gears. In both these situations, the EM assists the driving by providing torque via the even gears. It can be seen from Figure 6, that gear shifts will not be torque interrupt shifts, because the ICE will always be connected to the wheels through either the even or odd clutch.

Figure 7 shows the EV mode of 7DCTH. In EV mode, the ICE is off, both clutches are disengaged and the vehicle is driven via the even gear pairs.

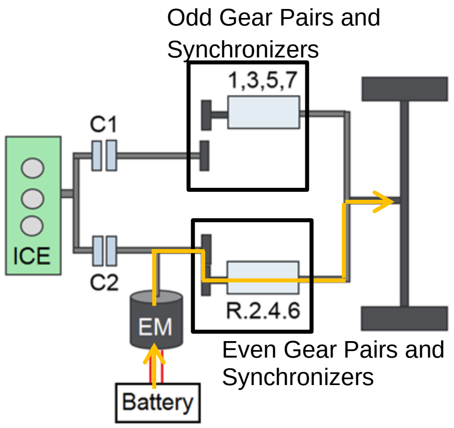

Figure 7 EV mode of 7DCTH

4. Torque Interrupt of a Hybrid DCT in EV Mode

The EV mode of 7DCTH shown in Figure 7 can be simplified, as shown in Figure 8. It can be seen that the simplified 7DCTH in EV mode is equivalent to a manual transmission.

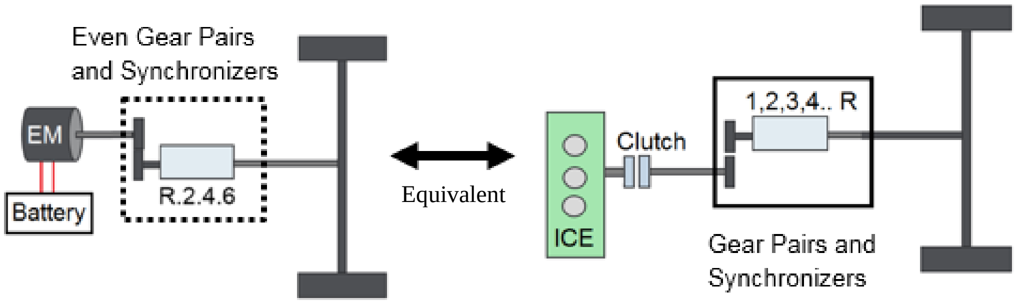

Figure 8 7DCTH and Manual Transmission

The equivalence of 7DCTH in EV mode to a manual transmission means that, in EV mode, 7DCTH will have ‘‘Torque Interrupt shifts’’.

In a manual transmission, the driver controls the gear stick and clutch and decides when a gear shift should be carried. Thus, the torque interrupt will not come as a surprise and the shift time will not bother the driver. However, in 7DCTH and in all computer controlled transmissions generally, as the shift is controlled by transmission software, it may occur when the driver is not expecting it. Thus, the torque interrupt may surprise the driver and, especially if the shift takes a long time, the driver will perceive it as a nuisance.

5. Reducing the Shift Time

A detailed model of the parts in the 7DCTH which are involved in a gear shift, in EV mode, is shown in Figure 9.

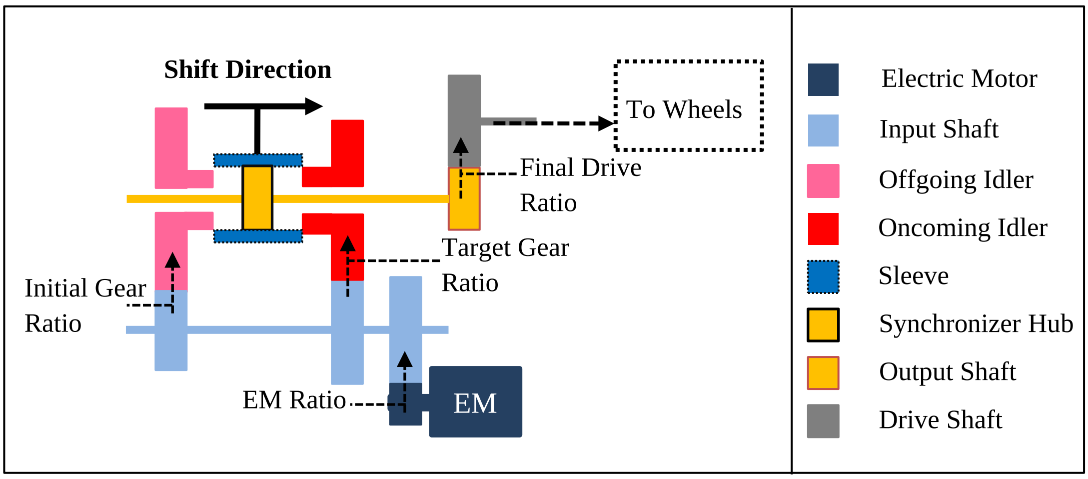

Figure 9 Driveline of 7DCTH in EV mode

Before the shift is ordered, the sleeve (shown in blue in Figure 9), will be connected to the offgoing idler (shown in pink). The torque from EM goes to the input shaft through the EM ratio, then through the initial gear ratio to the sleeve and finally to the synchronizer hub, which is connected to wheels. The following phases occur when a shift is ordered:

1. *Torque Ramp down*
   The EM torque being applied on the oncoming idler is reduced. Once the torque is zero the next phase starts.
2. *Sleeve to Neutral*
   The sleeve is moved in shift direction towards the oncoming idler, as shown in Figure 9, and is stopped when it is no longer in contact with the off-going idler
3. *Speed Synchronization between Sleeve and Gear*
   In the speed synchronization phase, the rotational velocity of the oncoming idler is matched to that of the sleeve.
4. *Sleeve to Gear engagement*
   Once the relative velocity between the oncoming idler and sleeve is zero, the sleeve is engaged with oncoming idler. Any torque applied to the idler will now be transferred via the sleeve to the output shaft.
5. *Torque Ramp up*
   Once the sleeve has moved a certain distance into the oncoming idler, the EM resumes its torque to drive the vehicle.

Thus, the total shift time is the time spent from the beginning of Phase 1 *Torque ramp down* to the end of Phase 5 *Torque Ramp up*.

6. Speed Synchronization between Sleeve and Gear

The greatest percentage of shift time is spent on Phase *3 Speed Synchronization between Sleeve and Gear*. Thus, to reduce shift time, the speed synchronization must be done as fast as possible. Speed synchronization in a hybrid DCT can be done in the following ways:

1. By using mechanical synchronizer
2. By using EM
3. By using both EM and synchronizer sequentially
4. By using both EM and synchronizer simultaneously

Paper A analyses the first three-speed synchronization methods.

The complete mechanical synchronizer in Figure 9 is shown in Figure 10a.

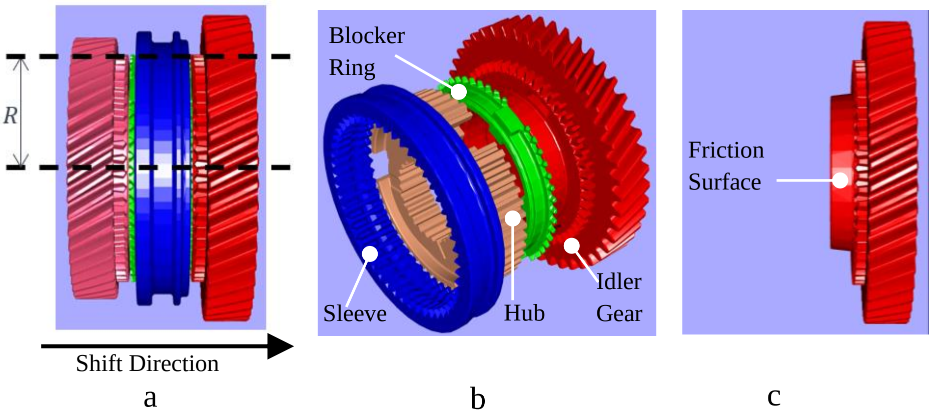

Figure 10 Mechanical synchronizer a) Complete Mechanical synchronizer b) exploded view of synchronizer c) Friction surface of Cone clutch

Figure 10b shows the exploded view of the mechanical components of the synchronizer. The friction surface on the idler gear is shown in Figure 10c. The friction between the blocker ring and the oncoming idler is used to synchronize the speed between the sleeve and the oncoming idler before the engagement.

Since the mechanical synchronizer is designed for a conventional DCT, the added inertia of the electric motor increases the shift time. If mechanical synchronizer is used for synchronization and synchronization time is required to be the same as in a conventional DCT, the life of the synchronizer will be reduced. By using the EM for synchronization, it is possible to achieve the same synchronization time as a conventional DCT, without additional wear of the synchronizers. However, at low temperatures the battery power drops. In those cases, the speed synchronization time with the electric motor increases significantly.

A high-level control algorithm in **Paper A** calculates how to minimize the time required for speed synchronization by considering the frictional work limits in the synchronizer, the maximum EM torque and the limits on battery power due to low battery temperatures.

Using the calculation method in **Paper A**, speed synchronization trajectories for oncoming idler for a typical upshift are shown Figure 11.

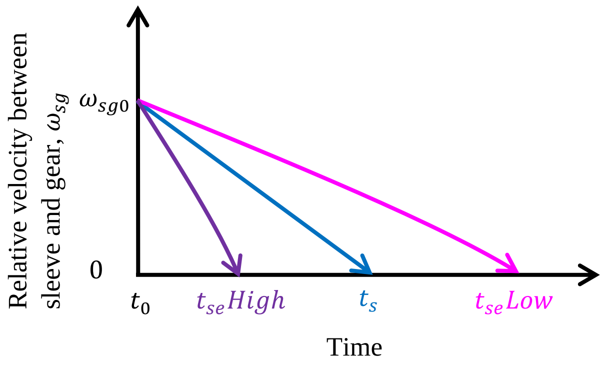

Figure 11 Speed synchronization trajectory for a typical Upshift

The y-axis shows the relative velocity between sleeve and gear, while the x-axis represents time. The time instance at which the relative velocity is zero is the synchronization time. ω_{sg0} is the relative velocity between the sleeve and gear before speed synchronization. The blue trajectory in Figure 11, is when the synchronizer is used for speed synchronization. Purple is when the EM is used with high battery power and magenta is when the battery power is low.

Figure 12 shows the supervisory algorithm for minimization of speed synchronization time.

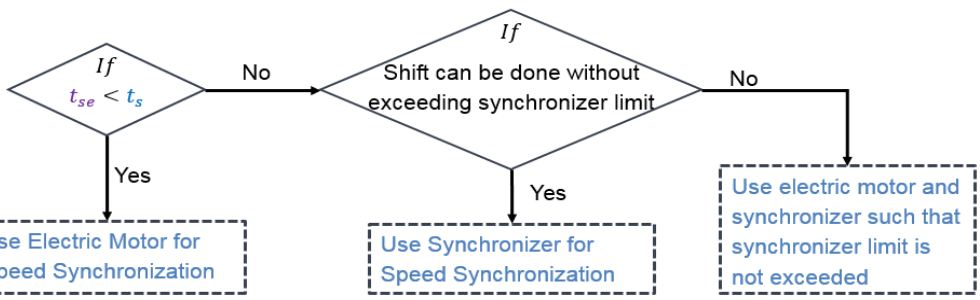

Figure 12 Supervisory algorithm for minimization of speed synchronization time

In Figure 12, t_{se} is the synchronization time using the electric motor at the present battery power and t_s is the synchronization time using the synchronizer.

Figure 13a depicts the situation in which a shift causes the synchronizer's frictional work limit to be exceeded while the battery power is low. Here, $\omega_{sg}L$ is the relative velocity limit corresponding to the frictional work limit of the synchronizer. Figure 13b shows the solution to minimize the synchronization time by sequential use of the EM and synchronizer developed in **Paper A**.

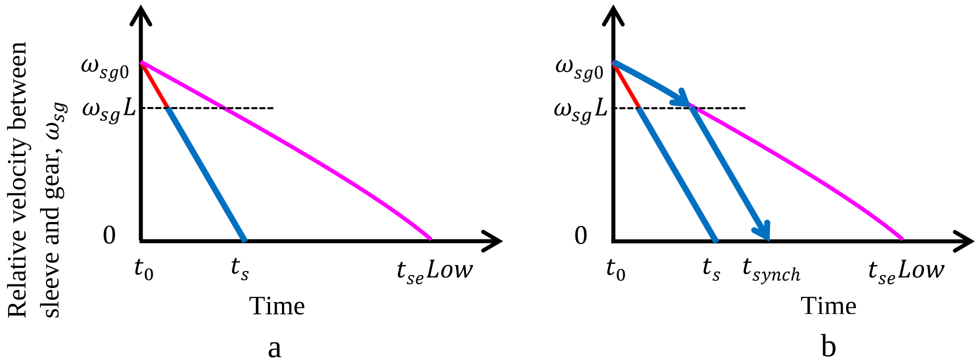

Figure 13 a) Speed synchronization when synchronizer limit is exceeded and low battery power b) proposed solution

It can be seen from Figure 13b (blue curve), that the synchronization time t_{synch} is less compared to using only the EM for synchronization while synchronizer limits are not exceeded.

7. Sleeve to Gear Engagement

As explained in **Paper B** *Sleeve to gear engagement* phase is responsible for noise and wear during gear shifts. The noise and wear come from contact between the sleeve and the idler gear dog teeth before phase *5 Torque ramp-up* starts. The contact can be described based on the alignment between sleeve teeth and idler gear dog teeth y_{sg} at a time t_{synch} when speed synchronization is finished. Figure 14 shows sleeve to gear engagement for two different values of $y_{sg}(t_{synch})$.

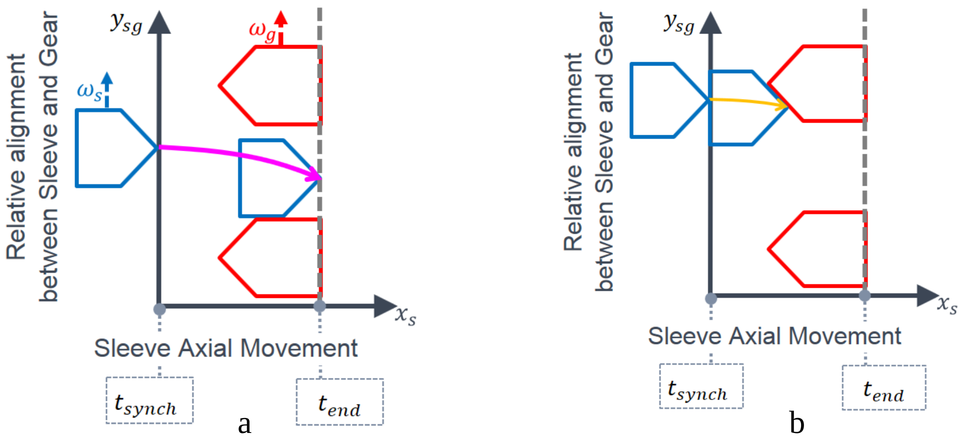

Figure 14 Teeth Contact during sleeve to gear engagement a) Ideal engagement without noise and wear and b) engagement with contact and noise/wear

As can be seen in Figure 14a, if the magenta trajectory is followed there is no contact between the sleeve and the idler gear dog teeth before time t_{end}, which represents the start of the *Torque Ramp Up* phase. However, if the sleeve follows the yellow trajectory in Figure 14b, there would be contact between the teeth and such a sleeve to gear engagement would lead to noise and wear. There are several different types of unwanted contacts between sleeve and gear during engagement. All are described and analysed in **Paper B**.

The detailed formulation of the trajectories shown in Figure 14 are shown in **Paper B**. Simulation results show that if, at time t_{synch}, the relative teeth alignment is a particular value i.e. $y_{sg}^*(t_{synch})$ the resulting sleeve to gear engagement is:

- Fastest
- Does not produce clonk or rattle
- Torque ramp-up starts simultaneously with the sleeve coming into contact with gear. Thus, contact between the sleeve and the gear is minimized and consequently wear in the transmission is minimized

Paper B also contains a detailed explanation of a newly developed ‘‘Dog teeth position sensor’’ which can measure the relative alignment between sleeve and idler gear teeth. This is a prerequisite for being able to start the engagement at the optimal relative teeth alignment. A model-based open-loop controller is also developed in **Paper B** that makes sure that $y_{sg}(t_{synch})$ is always the desired $y_{sg}^*(t_{synch})$.

The control algorithm is applied to the physical model of the system and simulations are run to see whether the contact force during the engagement has reduced. This shows that the noise/wear due to the engagement is minimized. Thus, it is important to model the contact forces between sleeve and gear. For this, AMESim’s 2D contact model, using a spring damper contact is used (as shown in Figure 15). The details of the method are given in [3].

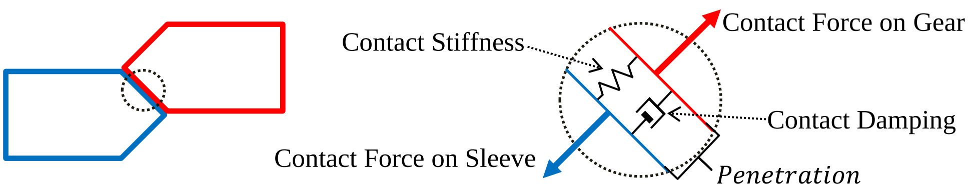

Figure 15   Contact force model between sleeve and idler gear teeth

8. Minimizing Speed Synchronization Time as well as Noise and Wear

To minimize speed synchronization time as well as noise/wear during shifts, speed synchronization and relative alignment between sleeve and gear must be controlled. The following sections describe the algorithms which can control these two states.

8.1 Model-based, open-loop control for minimization of noise and wear

The phase plane trajectory for speed synchronization is shown in Figure 16.

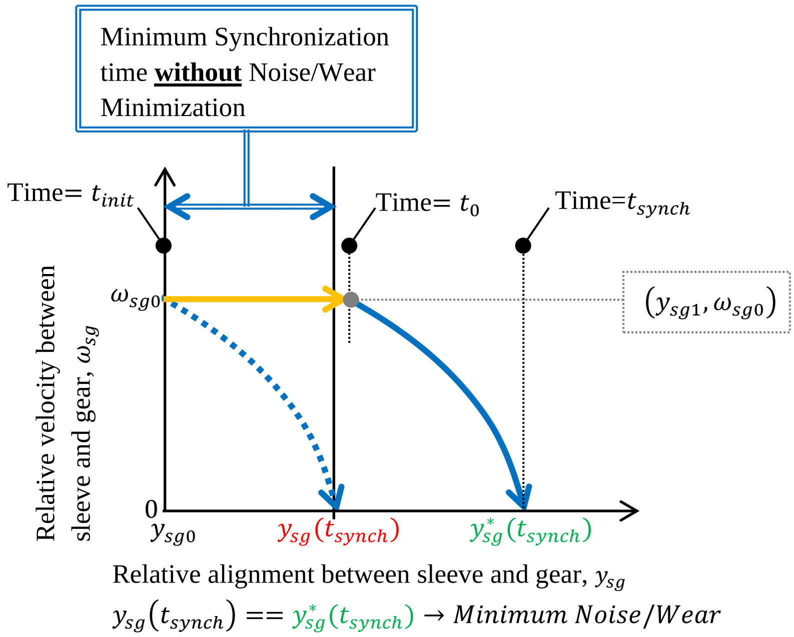

Figure 16 Speed synchronization and Open loop control

Note that Figure 16 and the proceeding figures covering speed synchronization do not show the different parts of the sequence in their correct proportions. The relative velocity between the sleeve and gear is shown on the y-axis in Figure 16 and goes to 0 from ω_{sg0}. The relative alignment between the sleeve and gear y_{sg} is shown on the x-axis. The synchronization done according to **Paper A** is shown as a dotted blue curve. At time t_{init}, when sleeve is at neutral, the speed synchronization is started. Since relative alignment is not considered in the control method in **Paper A**, in most gear shifts y_{sg} at time t_{synch} will not be equal to $y^*_{sg}(t_{synch})$, as indicated by the red text in Figure 16. Thus, by following the dotted blue curve the synchronization time is minimized while noise and wear are not.

In **Paper B,** a relative alignment y_{sg1} is calculated. If the speed synchronization is started at this point at time t_0 when y_{sg} is y_{sg1} then y_{sg} at time t_{synch} will become $y^*_{sg}(t_{synch})$, which will lead to noise-free engagement and minimum wear on the dog teeth,. This is indicated by the green text in Figure 16. The control algorithm is shown in Figure 17.

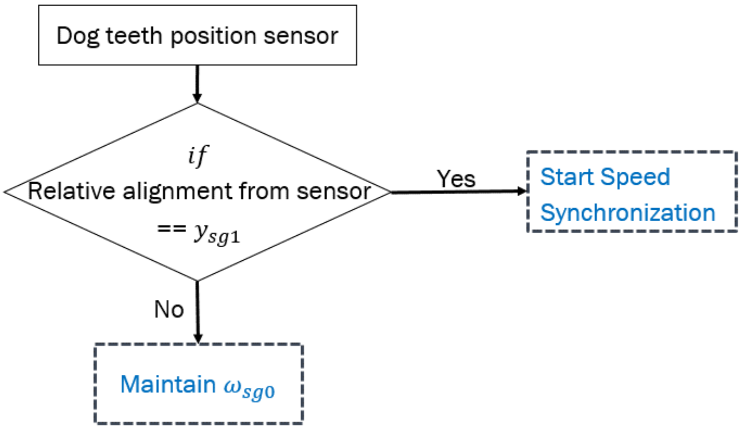

Figure 17 Control algorithm to Minimize Noise and wear

The speed synchronization trajectory resulting from the application of the algorithm in Figure 17 will be, as shown in Figure 18.

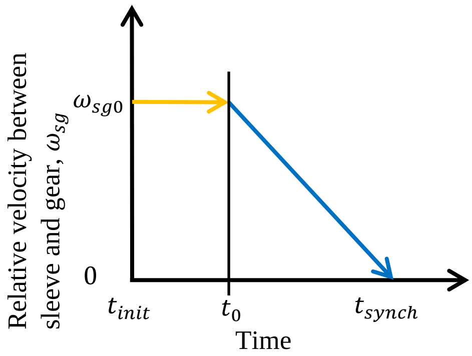

Figure 18 Speed synchronization trajectory for minimization of Noise/wear

As can be seen in Figure 18, the time interval between t_{synch} to t_0 will be the same as the ‘‘Minimum Synchronization time **without** Noise/Wear Minimization’’ in Figure 16. Thus, the synchronization is delayed by a time interval $t_0 - t_{init}$.

It should be noted that $t_{synch} - t_0 \cong 300ms$ for a nominal DCT and $t_0 - t_{init} \cong 3ms$ for the teeth geometry considered in this research, so the time added to avoid noise and wear is very small.

8.2 Feedback control for minimization of noise and wear

The control system developed in **Paper B** is a model-based, open-loop control system. Since the control action is taken at the start of speed synchronization, the control method in **Paper B** cannot avoid noise/wear if the system deviates from ideal trajectories during the process. **Paper D** proposes a feedback control method which aims to avoid noise/wear by continuously monitoring the sensor signals.

Figure 16 shows that if the speed synchronization does not start at the time when y_{sg} is equal to y_{sg1} then $y_{sg}(t_{synch})$ will not be equal to $y^*_{sg}(t_{synch})$. **Paper D** also discusses the fact that if the start of speed synchronization is delayed, it will still be possible to minimize noise/wear in the shift by increasing the speed synchronization time. The control algorithm that minimizes the synchronization time and noise/wear is described in section 8.3.

For the gear shifts which are part of the standard computer-controlled gear shifting algorithm, ω_{sg0} i.e. the relative velocity between gear and sleeve when the speed synchronization is started, is fixed. So, the model-based open-loop controller described in **Paper B** can be used to minimize noise/wear for such gear shifts. For gear shifts requested by the driver, known as Tiptronic shifts, ω_{sg0} is not fixed. To minimize noise/wear in Tiptronic shifts, model-based open-loop controller can be used but implementation will be simpler if a feedback control method is used.

In general, a feedback controller varies the control effort continuously to keep the system from deviating from the ideal trajectory. The controller input in **Paper D** is the synchronization torque request from either the electric motor or the mechanical synchronizer. It is better to keep the torque request at well-defined levels and vary the time intervals in which different torques are applied. This approach is easier to implement in the vehicle, so a switch mode controller is designed in **Paper D.**

Paper D defines a zone in the phase plane, as shown in grey in Figure 19. If the controller keeps the system within the grey zone, the noise/wear during the shift is guaranteed to be minimized.

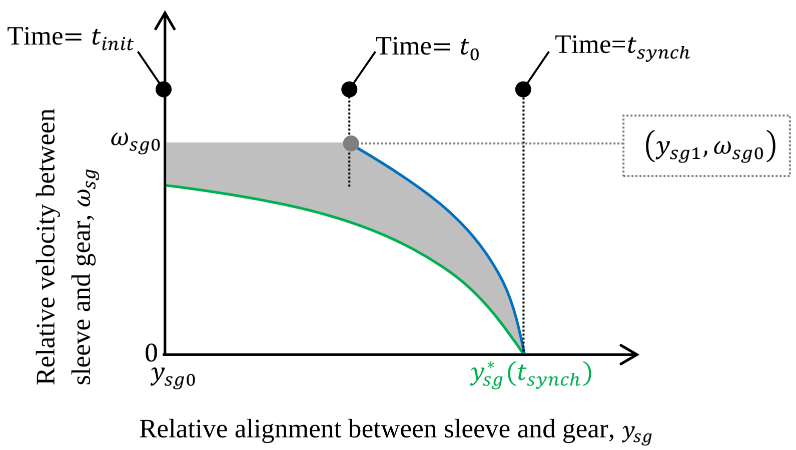

Figure 19   Zone in phase plane for feedback control

During the speed synchronization the trajectory of the synchronization is determined based on the speed and dog teeth position sensors. As shown in Figure 19 since the zone converges on $y_{sg}^*(t_{synch})$, it can be guaranteed that $y_{sg}(t_{synch})$ will always be equal to $y_{sg}^*(t_{synch})$. The zone can be implemented by describing its borders in two one-dimensional look-up tables in the control algorithm.

The top-level implementation of the feedback control law is shown in Figure 20. The inputs to the feedback control law are: relative speed from speed sensors; relative angular alignment from position sensors in the transmission; and the zone definition from Figure 19.

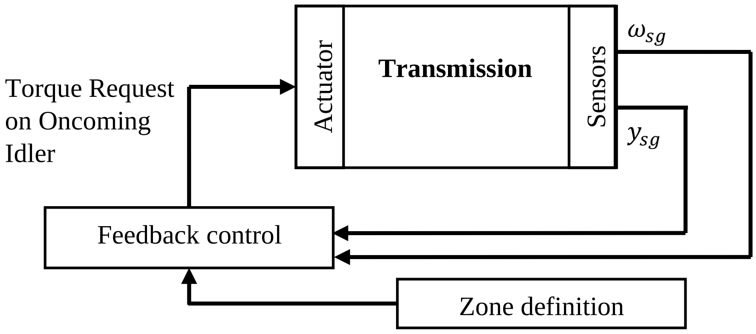

Figure 20 Implementation of feedback control

Phase plane trajectory for speed synchronization for two different values of $y_{sg}(t_{init})$ after the application of feedback control law in Figure 20 is shown in Figure 21, indicated by the purple and dotted red curve.

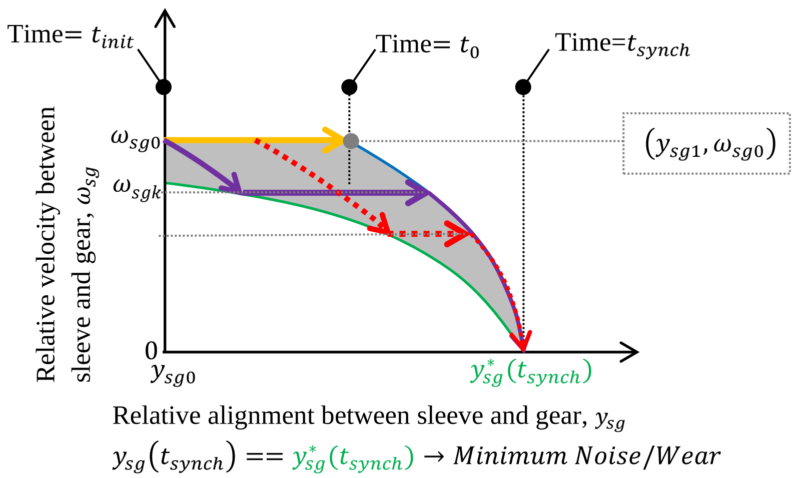

Figure 21 Speed synchronization and Feedback control

As shown by the purple trajectory in Figure 21, the speed synchronization is started at time t_{init} instead of waiting until time t_0 as shown by the yellow trajectory**.** When the feedback control system detects that the trajectory has hit the zone's lower boundary, the synchronization torque is switched such that a particular relative speed ω_{sgk} is maintained while the relative angular alignment between sleeve and gear y_{sg} changes. Once the control system detects that the trajectory has hit the upper boundary of the zone, the control system changes the synchronization torque back to the maximum value and speed synchronization starts again.

8.3 Minimization of speed synchronization time, noise and wear

Paper C discusses how the time interval $t_0 - t_{init}$ in Figure 18 can be minimized. This problem is formulated as *Time-optimal control*. The goal of time-optimal control is to adjust the relative alignment from y_{sg0} to y_{sg1} in the minimum time. If ω_{sg} is plotted with respect to time, as shown in Figure 22, then the area under the curve between time t_{init} and t_0 will be equal to the corresponding required change in relative angle. This is $(y_{sg1} - y_{sg0}) \div R$, where R is the effective radius of dog teeth in synchronizer, as shown in Figure 10.

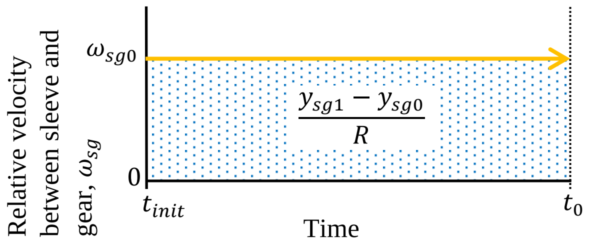

Figure 22 Velocity profile at start of speed synchronization in open loop control

The time it takes to adjust the relative angle, that is, the interval between time t_{init} and t_0, can be decreased by changing the velocity profile, as shown in Figure 23.

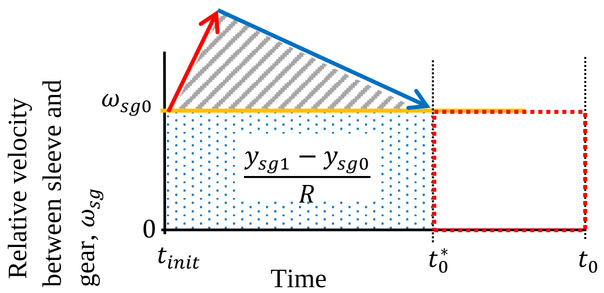

Figure 23 Velocity profile at start of speed synchronization in time-optimal control

As shown in Figure 23, the velocity profile is changed by first increasing the velocity from ω_{sg0} to a certain level (as shown by the blue curve) and then decreasing it back to ω_{sg0} (as shown by the red curve). If the area of the red dotted rectangle in Figure 23 is equal to the area of the hatched triangle then the required change in relative angle, such as $(y_{sg1} - y_{sg0}) \div R$, is achieved in a smaller time interval $t_0^* - t_{init}$.

Then at t_0^*, if speed synchronization is started, y_{sg} at time t_{synch} will become $y_{sg}^*(t_{synch})$, leading to noise-free engagement and minimum wear of dog teeth, as mentioned before.

The minimum value of the time interval $t_0^* - t_{init}$, corresponds to the maximum value of the area of dotted red rectangle. As mentioned before, this is equal to the area of the hatched triangle. So, $t_0^* - t_{init}$ will be minimum if the area of the hatched triangle is maximum. The area of the hatched triangle will be maximum if the slope of the increasing red curve and slope of the decreasing blue curve are maximum.

Physical meaning of maximizing relative velocity slopes means applying maximum torque to the idler gear. From Figure 23 it can be seen that first a maximum torque must be applied, and that will increase the relative velocity for a short time, and then maximum negative torque must be applied, and that will decrease the relative velocity.

Applying maximum input in either direction is the essence of Bang-Bang control, which is generally a solution to time-optimal control problems. The general proof and implementation of the complete feedback control are given in **Paper C**. Figure 24 shows the top-level implementation of the feedback control law.

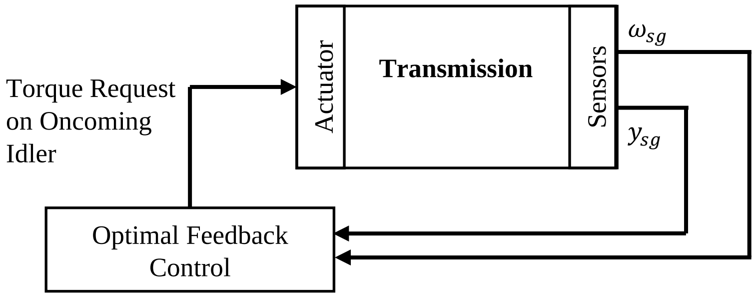

Figure 24   Implementation of Time-optimal control

Figure 25 shows the speed synchronization trajectory after applying the time-optimal control from Figure 24.

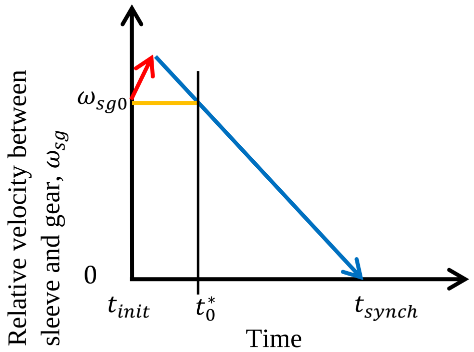

Figure 25   Speed synchronization trajectory for minimization of synchronization time and Noise/wear

9. Summary of Control Methods for Speed synchronization with minimization of Noise and Wear

Figure 26 shows a summary of all four control methods presented. Starting from a certain ω_{sg0}, there are four paths that can be taken.

1. Starting with speed synchronization immediately by following the dotted blue curve
   a. Speed synchronization time is minimized
   b. Noise/Wear is not minimized
2. Maintaining ω_{sg0} until a time t_0 when relative teeth alignment is y_{sg1}, hence following yellow curve, then starting speed synchronization, hence following blue curve.
   a. Speed synchronization time is not minimized
   b. Noise/Wear is minimized
3. Starting the feedback control decrease ω_{sg}, following the purple curve, if the trajectory hits the lower boundary of the zone, maintain ω_{sg} until the trajectory hits the upper boundary of the zone, then start speed synchronization again, hence following the purple curve.
   a. Speed synchronization time is not minimized
   b. Feedback control implies that deviations from ideal trajectories will be handled
   c. Noise/Wear is minimized
4. Starting feedback control, ω_{sg} will first increase, following the red curve, and then decrease, following the blue curve.
   a. Speed synchronization time is minimized
   b. Noise/Wear is minimized

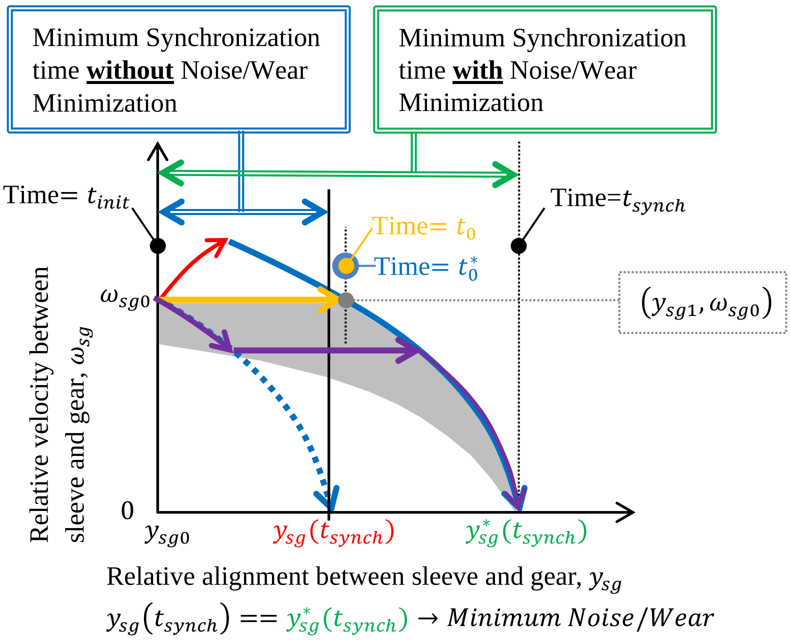

Figure 26 Minimization of synchronization time and noise/wear

Part 2: Control of Dedicated Hybrid Transmission

A dedicated hybrid transmission (DHT) contains an internal combustion engine (ICE) and one or more traction electric motors. DHTs are a cost-effective way of introducing hybridization because, with ICEs, the battery size required for the same range is smaller than that of a fully electric vehicle.

Figure 27 shows a DHT concept chosen at China Euro Vehicle Technology AB (CEVT). ICE is connected to a dual mass flywheel (DMF) which, in turn, is connected to the P1 electric motor. The P1 electric motor is connected to the primary side of the dog clutch (shown in red in Figure 27). The secondary side of the dog clutch (shown in green) is connected to the P3 electric motor. This is then connected to wheels via a gear ratio.

While driving the vehicle can be in the following modes

1. Pure Electric
2. Series Hybrid
3. Parallel Hybrid

In pure electric mode (EV), the engine is off, the dog clutch disengaged and P3 is providing driving torque to the wheels. Figure 27a shows the power flow from the battery to the P3 motor using blue arrows. When the state of charge in the battery is low the vehicle is shifted to series hybrid mode. If the engine is off, the P1 motor can take power from the battery and act as a starter motor. Once the engine is running, it is used as a range extender and the battery is charged by P1 motor. This is shown in Figure 27a by the yellow arrows.

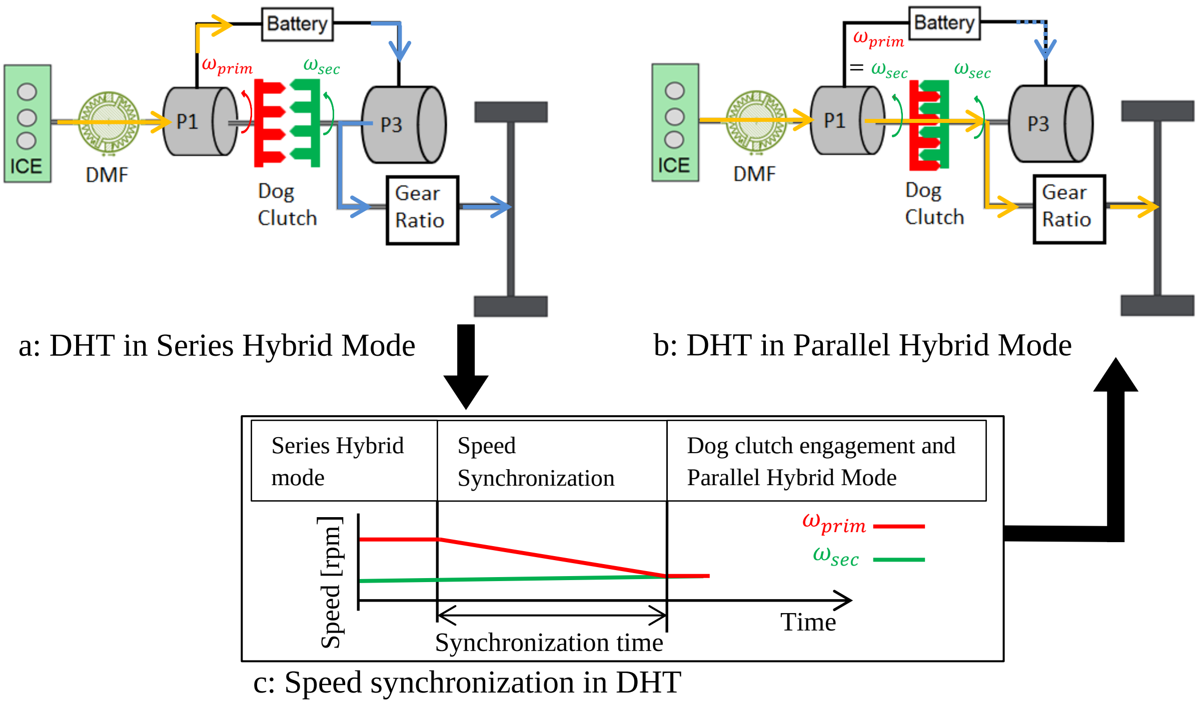

Figure 27 Mode switch in DHT a) Series Hybrid Mode b) Parallel Hybrid Mode c) Speed synchronization

When the vehicle speed is larger than a particular value v_1, the vehicle should be in parallel hybrid mode for the sake of efficiency. In parallel mode the dog clutch is engaged, thus connecting the ICE to the wheels as shown in Figure 27b. Since the vehicle is shifted to parallel mode for efficiency reason rather than due to low battery power, sufficient battery power will be available for the P3 motor to provide some of the driving torque as shown in Figure 27b by the dotted blue arrow.

In series mode, the primary and secondary sides of the dog clutch (shown in Figure 27a in red and green respectively) will be moving at different velocities. Before the dog clutch is engaged and the vehicle shifted from series hybrid mode to parallel hybrid mode, the speed across the dog clutch needs to be synchronized. In other words, the primary side velocity ω_{prim} and secondary side velocity ω_{sec} in Figure 27a need to be matched. The speed synchronization in DHT (shown in Figure 27c) is the control problem discussed in this thesis.

10. Speed Synchronization in Dedicated Hybrid Transmission

The speed synchronization shown in Figure 27c is important for noise/wear reduction in the dog clutch during a mode switch.

Figure 28 shows the traction effort curve of the vehicle, with vehicle speed on the x-axis and traction torque at the wheels on the y-axis. Figure 28a shows the series hybrid mode, in which the limits are defined by P3 electric motor power.

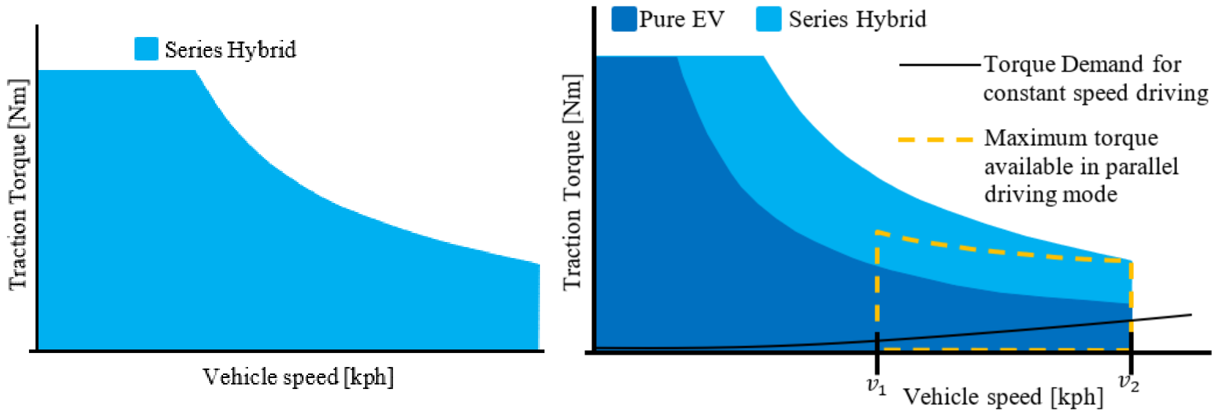

a: DHT in Series Hybrid Mode

b: DHT in Series Hybrid and EV mode

Figure 28 Traction Torque curve in a) Series Hybrid and b) Series hybrid and EV mode with torque demands

In EV mode the limits are defined by the maximum battery power, as shown by the dark blue area in Figure 28b. Figure 28b shows that the maximum battery power is lower than the P3 electric motor power. In series hybrid mode, the power is supplied to the P3 motor from the ICE via P1 which acts as a generator. This is a special case for the DHT being studied, with the battery size kept small to keep the cost low.

The yellow dashed line in Figure 28b represents the maximum torque available to the wheels in parallel driving mode. It is the sum of the maximum engine torque and torque from the P3 motor provided by the limited battery power.

The torque delivered to wheels in parallel driving mode (shown in Figure 27b) can be calculated by drawing ICE torque map, after multiplying by the gear ratio (on the traction effort map in Figure 28), as shown in Figure 29.

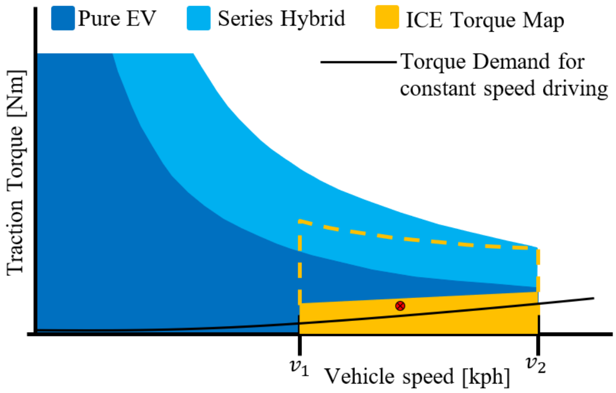

Figure 29 Traction effort curve with engine operating point in series mode

The red dot in Figure 29, represents the engine speed and torque used when vehicle is in series hybrid mode. Before the vehicle velocity reaches v_1, the engine would be running at this point of optimum efficiency and the P1 motor would be in generator mode.

Figure 27a shows that in series mode the secondary side velocity follows the vehicle speed and the primary side velocity will be equal to the engine speed. Thus, for speed synchronization engine speed, denoted by the red dot in Figure 29 needs to be reduced.

Figure 30 is a magnified view of Figure 29, for a slow acceleration driving case. The torque demand for slow acceleration is shown by the dashed black line**.** When the vehicle speed is greater than a particular speed v_{init}, speed synchronization is started.

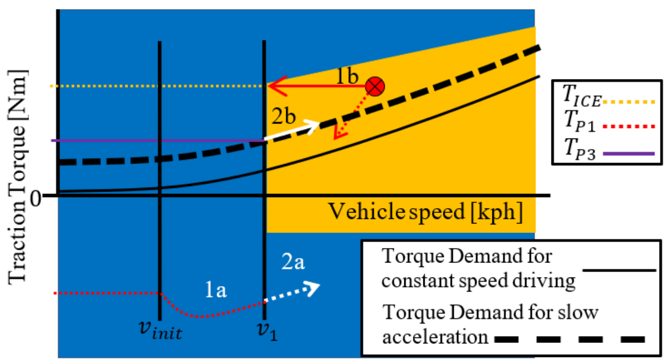

Figure 30 Mode switch for slow acceleration

As shown in Figure 30, the speed synchronization (a reduction in engine speed in this case) may be done either by cutting the fuel to the engine as shown by the dotted red arrow, or by applying a braking torque to the engine via the P1 electric motor, as shown by the solid red arrow. Since speed synchronization between the primary and secondary sides of the dog clutch is the aim, it is much more controllable if braking torque from the P1 motor is used, rather than letting the primary side speed reduce under friction by cutting the fuel to the engine.

In Figure 30, when the vehicle velocity is less than v_{init}. The P1 motor is running in generator mode and applying a constant braking torque to the engine. When the vehicle speed is greater than v_{init}, a braking torque from the P1 motor is applied (as denoted by sequence 1a in Figure 30). This braking torque is calculated by the feedback controller explained in **Paper E**. It reduces the primary side velocity and, hence, the engine speed as denoted by sequence 1b in Figure 30. It should be noted that sequences 1a and 1b are simultaneous.

After the dog clutch engagement, the torque at the wheels will be the sum of the torque from ICE and the P1 and P3 motors. To maintain smooth acceleration of the vehicle during the mode shift, the torque from all sources needs to be managed such that the torque demand for slow acceleration is met during the entire mode shift.

By the end of speed synchronization and during dog clutch engagement, the torque request from the P1 motor will be approximately equal to T_{ICE}, as shown in Figure 30. In Figure 30, torque ramp-up is denoted by sequence 2. The smooth acceleration profile may be achieved for instance by keeping the torque from the P3 electric motor, T_{P3} constant and smoothly reducing the braking torque T_{p1} from the P1 electric motor, as shown by the white dotted curve 2a in Figure 30. Consequently, the torque applied at the wheels will follow the solid white curve 2b and the torque demand for slow acceleration driving will be met.

Figure 31, shows a magnified view of Figure 29 for a particular acceleration maneuver, with high acceleration. It should be noted that, in general, a mode switch from series to parallel will normally not be done during acceleration maneuvers unless the acceleration is very low, as in Figure 30. The purpose of the following discussion is to demonstrate that, if the situation requires, a mode switch under high acceleration is possible by using the speed synchronization method described in **Paper E**.

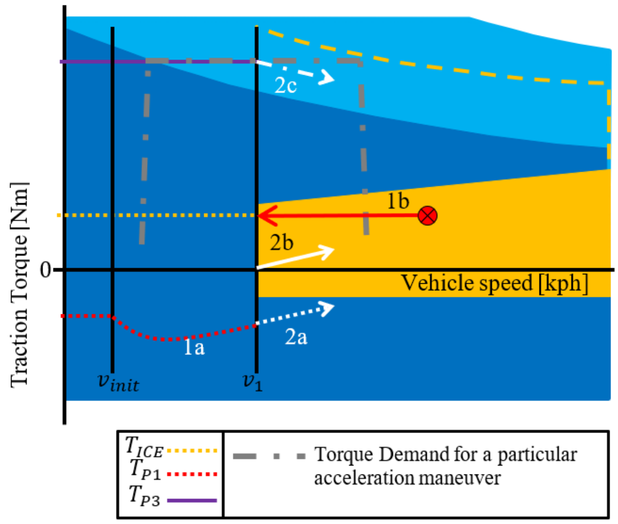

Figure 31 Mode switch for a particular acceleration maneuvre

When the vehicle speed is greater than the calibratable speed v_{init}, the speed synchronization is started by applying the braking torque T_{P1} on the engine using the P1 electric motor as shown by sequence 1a in Figure 31. Until the vehicle shifts to parallel driving mode, the torque demand at the wheels is met by the P3 electric motor by supplying the torque T_{P3} as shown in Figure 31. Once the speed is synchronized across the dog clutch at vehicle speed v_1 (as shown by sequence 1b), the dog clutch can be engaged with minimum noise and wear.

After engaging the dog clutch, the braking torque supplied by the P1 electric motor is reduced (as shown by the dotted white curve 2a in Figure 31). Consequently, the torque from the primary side of the dog clutch will increase, as shown by the solid white line 2b in Figure 31. Since extra torque from the engine and P1 motor is now delivered to the wheels, the torque from the P3 motor can then be reduced, as shown by the dot-dash white line 2c in Figure 31.

From the above section, it can be concluded that the first phase in the mode switch (speed synchronization) is not time-critical. Depending on the power available to the P1 electric motor for applying braking torque, the calibratable speed when the speed synchronization starts v_{init} in Figure 30 and Figure 31 can be changed. From Figure 31, it can also be seen that, even for an acceleration maneuver, the torque from the P3 electric motor is sufficient to meet the torque demand and that the mode switch to parallel driving is only made because of efficiency requirements. Unlike transmissions in conventional powertrains, in which speed synchronization during mode switch is a time-critical problem (in terms of meeting the torque request), the controller design in **Paper E** will focus on speed synchronization and dog clutch engagement without noise and wear.

11. Engagement Test Results for Dedicated Hybrid Transmission

In normal vehicle operation, the dog clutch is engaged after speed synchronization. However, in a lab, the tests are run by measuring the instantaneous peak acceleration produced in a dog clutch by engaging it at different relative velocities. Figure 32 shows the test results reported in **Paper E**.

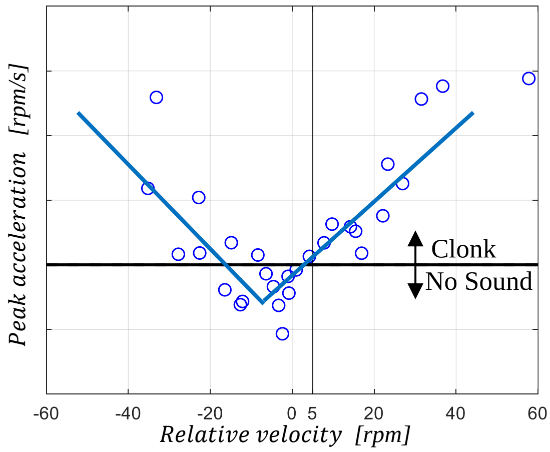

Figure 32 Lab Tests for dog clutch engagement at different relative velocities

Figure 32 shows that if the relative velocity is between 5 and approximately -20 rpm, the instantaneous peak acceleration would be so low that there would be no clonk sound. The dark blue lines in Figure 32 show the trend.

Theoretically, the test results must be centred around zero since the peak acceleration produced by an impact is directly proportional to the relative velocity at the moment of impact (shown by the red trendline Figure 33). However, the test results are off-centre, as shown by the blue trendline. This is because the relative velocity in the tests was measured before the actual impact.

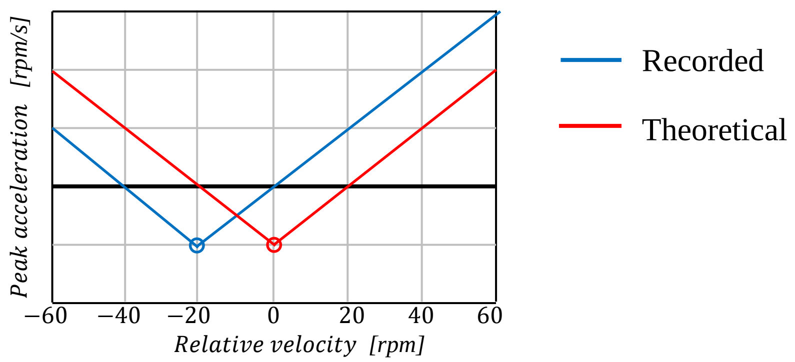

Figure 33 Theoretical and recorded peak acceleration trend wrt relative velocities

As shown in Figure 33 the relative velocity measured before impact is -20 rpm as shown by the blue circle. This generates the lowest peak instantaneous acceleration value in the transmission at impact. Theoretically, the lowest peak instantaneous acceleration value must be generated by the 0 rpm relative velocity, as shown by the red circle in Figure 33. It may be concluded that between the time the relative velocity is recorded as -20 rpm and the time when the actual impact happens (and the instantaneous peak acceleration is recorded), the drag torque in the transmission changes the relative velocity to 0 rpm.

12. Modeling Dual-Mass Flywheels in Hybrid Transmissions

To develop the control algorithm explained in **Paper E** requires a simulation model of the DHT. Calculating the damping of the DMF in automotive transmissions is always a challenge, as this is not usually provided by DMF suppliers. To find a suitable realistic value to be used in the simulation models, a complete powertrain simulation model of the DHT as shown in Figure 34 is used in this thesis.

The power train model can then be used to simulate various operating points of the vehicle such as, idle, launch, start, tip in/back out etc. as shown in [4]. The simulation results can then be compared to the test data for particular operating points, and then a suitable damping value for the DMF can be estimated.

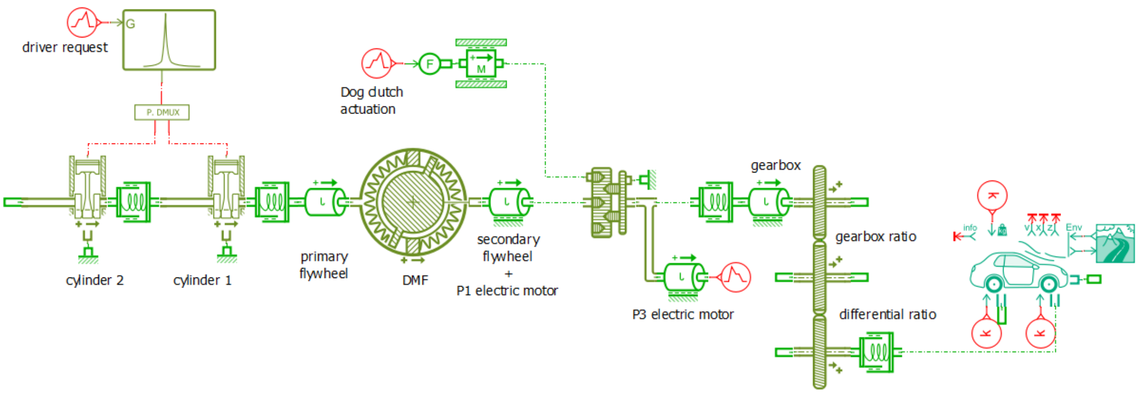

Figure 34 Powertrain model for DMF modeling

Figure 35 shows the fluctuations on the secondary side of the DMF for two different values of damping when the vehicle is idling.

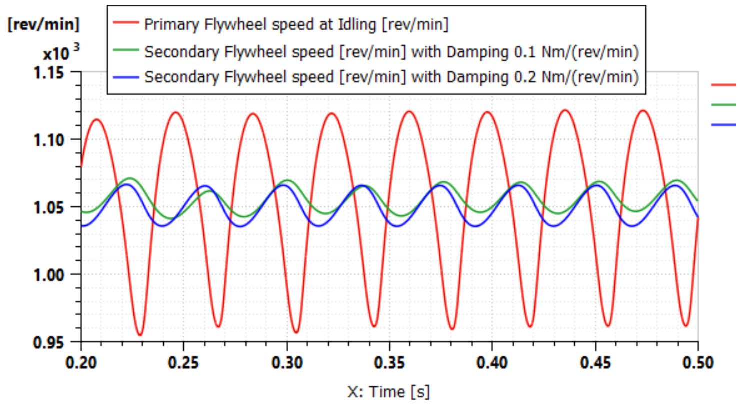

Figure 35 Speed fluctuations with two different damping values for the DMF

By running batch simulations with different damping values and collecting the amplitude of speed fluctuations on the secondary side, a plot similar to [5] may be drawn (as shown in Figure 36). By comparing the amplitude of fluctuation with the vehicle test data, an appropriate damping value may be chosen for use in simulation modeling and control method development.

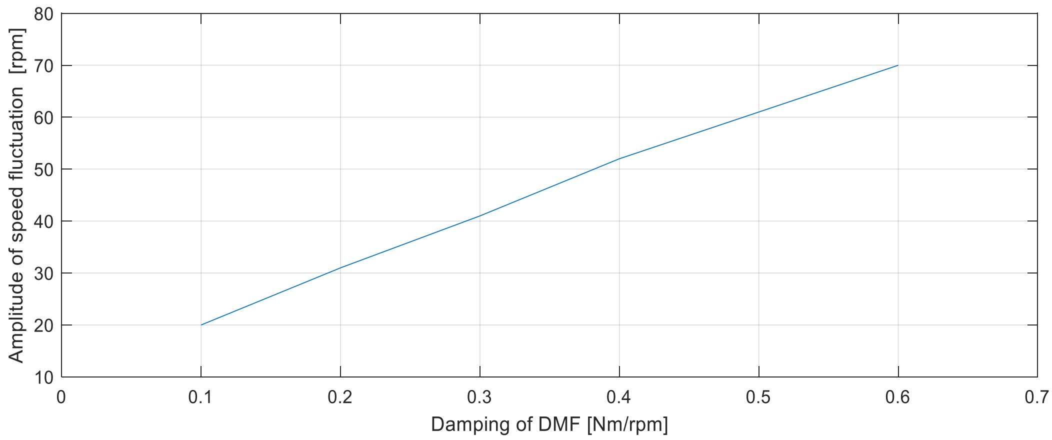

Figure 36 Influence of DMF damping on speed fluctuations of secondary side

Conclusions

This thesis has made a detailed examination of shift time, noise and wear during gear shifting, as these are important to gear shift quality. Control algorithms for their minimizations are designed and implemented.

Using the control methods in this thesis, a 7DCTH will have the minimum time for torque-interrupt shifts, thus improving the shift quality of the vehicle. The noise/wear in the synchronizers during the shift will also be minimized, thus increasing the life of the transmission and the passenger comfort. Since 7DCTH has carry-over components from the 7DCT already in production, the production costs of the hybridization will be low.

Paper A shows how speed synchronization time in 7DCTH can be improved by using both synchronizer and EM.

Paper B shows how transmission noise and wear can be minimized by using the dog teeth position sensor. The paper demonstrates that speed synchronization time will not increase significantly if noise and wear are minimized. The algorithm can be extended to conventional DCTs with very small modifications.

Paper C calculates the absolute minimum time if both speed synchronization time and noise/wear is to be minimized. The implemented feedback controller is suitable for dog clutch systems in general. Thus, the application area can be extended to systems other than hybridized transmissions.

Paper D presents a feedback control approach, where the controller is designed in the phase plane, hence making its implementation quite simple. Not only can the feedback control algorithm minimize noise/wear in computer-controlled shifts but also in Tiptronic shifts ordered by the driver. The application of the algorithm can be extended to synchronizer and dog clutch systems in general.

Dog clutch systems generally have lower manufacturing costs than mechanical synchronizers. Using the control methods in this thesis the mechanical synchronizers in 7DCTH can be replaced by dog clutches, if there is sufficient battery power available for speed synchronization.

A DHT provides hybridization and cost-effectively meets the required emission criteria by using a relatively small battery size and an ICE running at an optimal operating point for most of the driving time. The DHT concept presented in this thesis shifts from series hybrid to parallel hybrid mode at high vehicle speeds. **Paper E** presents an LQI controller formulation for speed synchronization of dog clutches in a DHT. The LQI controller is capable of minimizing noise/wear in the DHT during mode switch by minimizing the speed difference between the two sides of the dog clutch affected by the disturbance from the combustion torque of the engine. **Paper E** also provides an algebraic method for tuning LQI controllers based on physical parameters of the system and performance requirements. Thus, the controller tuning method can be used also for systems other than the dog clutch being investigated.

The control methods in this thesis were developed by keeping the existing control hardware and software in mind. This meant that all complex calculations were done offline and the control algorithms to be implemented in the embedded system were kept simple. Using this approach, optimum performance from the mechanical synchronizer or dog clutch system can be achieved, without extending the vehicles' existing control system.

Beyond transmissions, dog clutches are used as connect/disconnect mechanisms in other parts of the vehicle. The control methods described in this thesis are developed by keeping that in mind, so the control methods, although developed for transmissions, can be extended to noise/wear minimization for dog clutch systems in other applications as well.

Future work

1. This thesis did not examine the use of an EM and synchronizer simultaneously for speed synchronization, something which could potentially lead to even better results.
2. The dog teeth position sensor presented in **Paper B** needs a very high sampling rate to work. Using alternate methods of sensing dog teeth position, such as the one presented in [6] will be a topic of future research.
3. The algebraic weight selection for LQI controllers presented in **Paper E** may be further improved by using non-diagonal forms of the Q matrix.

References

[1] "Cost, Effectiveness, and Deployment of Fuel Economy Technologies for Light-Duty Vehicles," The National Academies Press, Washington, DC, 2015.

[2] T. S. Y. Z. Manish Kulkarni, "Shift dynamics and control of dual-clutch transmissions," *Elsevier Journal of Mechanism and Machine Theory,* no. 42, pp. 168-182, 2007.

[3] B. Wu and C. Chen, "Influence of the Sleeve Teeth Shape Parameters on the Shifting Process of Automated Manual Transmission for Electric Vehicles," *SAE International Journal of Electrified Vehicles,* vol. 9, no. 2, pp. 133-142, 2020.

[4] A. Fidlin and R. Seebacher, "DMF simulation techniques," LuK SYMPOSIUM, 2006.

[5] G. Wu and G. Zhao, "Parameter influence law analysis and optimal design of a dual mass flywheel," *International Journal of Mechanical System Dynamics,* vol. 2, pp. 165-177, 2022.

[6] Q. Kong, "Calibration and Estimation of Dog Teeth Positions in Synchronizers for Minimizing Noise and Wear during Gear Shifting," KTH, School of Industrial Engineering and Management (ITM), Stockholm, 2020.